AR-009-732

DSTO-TR-0357

DSTO

Vibration Isolator Test Facility

J.D. Dickens and C.J. Norwood

19970307 115

D E P A R T M E N T ◆ O F D E F E N C E

DEFENCE SCIENCE AND TECHNOLOGY ORGANISATION

Mar 17

Vibration Isolator Test Facility

J.D. Dickens and C.J. Norwood

Ship Structures and Materials Division
Aeronautical and Maritime Research Laboratory

DSTO-TR-0357

ABSTRACT

This report details the development of a vibration isolator test facility at the Aeronautical and Maritime Research Laboratory. The test facility was designed to investigate the acoustic transmission characteristics of resilient vibration isolating mounts for shipboard machinery. The characteristics of the isolators are described in terms of their four-pole parameters. Features of the test facility include the capability to sense low level motion and the provision of a variable pre-load up to 60 kN. A modal analysis was conducted with the boundary conditions that are experienced in an actual test situation. This revealed details concerning the influence of structural modes on the test measurements, and led to location of the sensing accelerometers which permitted data to be obtained out to 1 kHz with confidence. This report also describes the testing of a typical ship machinery mount in the test facility by determining the four-pole parameters of the vibration isolator.

RELEASE LIMITATION

Approved for public release

DEPARTMENT OF DEFENCE

◆

DEFENCE SCIENCE AND TECHNOLOGY ORGANISATION

Vibration Isolator Test Facility

Executive Summary

The vibratory power transmitted from a machine to its foundation, through the machine's vibration isolators, is dependent on the dynamic properties of the foundation, the machine and the isolators. A knowledge of these frequency dependent properties is vital for the acoustic signature management of naval surface ships and submarines.

The stiffness and damping properties of vibration isolators vary with both pre-load and frequency. In addition, standing waves can be set up within an isolator which reduces its effectiveness at those frequencies. It is therefore necessary to determine the isolator's properties at the pre-load conditions experienced in service. Any performance measure should also be independent of the test procedure, so that it is universally applicable. The transfer impedance has traditionally been used to describe dynamic performance of vibration isolators, but this measure is only applicable within the low frequency range where the isolator behaves like a massless spring.

A more complete description of an isolator's dynamic properties is provided by the four-pole parameters, which relates the forces and velocities between the input and the output. The vibration isolation for any situation may be determined from a knowledge of the four-pole parameters and the mobilities of the structure. The dynamic description of the isolator in terms of the four-pole parameters is derived in this report, and this is compared to the more traditional descriptions of dynamic stiffness and transfer impedance.

The test procedures necessary to measure the four-pole parameters of an isolator require it to be mounted between two large masses and excited over the frequency range of interest. A detailed description of the test procedures and the development of a test facility for the measurement of the four-pole parameters is provided. Results of measurements on a standard commercial isolator are used to show the importance of the different parameters and provide some representative results.

Authors

J.D. Dickens
Ship Structures and Materials Division

John Dickens graduated from the University of Tasmania in 1972 with an engineering honours degree. His career with the Defence Department commenced in 1978 and he has worked in a wide range of research and development areas involving weapons, ammunition, wheeled and tracked vehicles, ships and submarines. In 1992 he joined the Noise and Vibration section of the AMRL. He is currently employed as a Senior Research Engineer and is undertaking research into the noise and vibration control of machinery sources onboard ships and submarines.

C.J. Norwood
Ship Structures and Materials Division

Chris Norwood graduated with a degree in Mechanical Engineering in 1975 and was awarded a MEngSci in 1977 from Melbourne University. After working for a year in industry and four years as a research engineer at MRL and Loughborough University (UK), from where he received an MSc in 1980, he taught at Victoria University of Technology for eight years. He joined MRL in 1990 and has worked on the reduction of ship and submarine noise and vibration. His current position is Senior Research Engineer in the Ship Structures and Materials Division.

Contents

1. Introduction

The vibratory power transmitted from machinery mounted on vibration isolators depends upon the dynamic properties of the foundation, the machinery mounting point and the vibration isolation mounts. A knowledge of the frequency dependent dynamic properties of vibration isolators is necessary in order to be able to predict their isolation performances. For naval surface ship and submarine applications, determination of the vibration transmission characteristics is vital for acoustic signature management.

Most isolators contain elastomeric material, the stiffness and damping properties of which are both frequency and pre-load dependent. In addition it is possible for standing waves to be set up within the isolator at certain frequencies, which greatly reduce its effectiveness at those frequencies. It is therefore necessary to determine the isolator properties under the pre-load conditions and frequency range experienced in normal operation.

The transfer impedance or mobility of an isolator has traditionally been used to describe its dynamic properties and provide a measure of its isolation performance. This measure does not necessarily provide a full description and may also be dependent upon the test conditions. An alternative description is provided by the four-pole parameters, which relate the force and velocity above the isolator to the force and velocity below. The significance of the four-pole parameters description is that it provides a measure of the isolator dynamic properties which is not dependent upon the measuring set-up, and it can be used to give an estimate of the isolator effectiveness.

A vibration isolator test facility was developed at the Aeronautical and Maritime Research Laboratory to measure the frequency dependent vibration transmission characteristics of flexible isolation mounts used for machinery onboard ships and submarines. In this report the description of the isolator dynamic properties in terms of its four-pole parameters is developed and the experimental determination of these is outlined. The Aeronautical and Maritime Research Laboratory test facility is described in detail and sample results for a commercially available isolator are provided.

2. Vibration Isolator Properties and Performance

The four-pole parameters may be used to characterise the dynamic properties of anti-vibration mounts [1] - [7]. An anti-vibration mount may be modelled as the linear mechanical system shown in Fig. 1. The instantaneous input force and velocity are $\tilde{F}_1$ and $\tilde{V}_1$, and the instantaneous output force and velocity are $\tilde{F}_2$ and $\tilde{V}_2$, respectively. Consider that the system is linear and has motion described sinusoidally in time with a frequency of ω. Using frequency domain notation the forces and velocities may be expressed at time t as:

$$\tilde{F}_1(\omega, t) = F_{10}(\omega).e^{j.(\omega.t+\varphi_1)} \qquad \text{and} \qquad \tilde{F}_2(\omega, t) = F_{20}(\omega).e^{j.(\omega.t+\varphi_3)} \qquad \text{(1a, b)}$$

$$\tilde{V}_1(\omega, t) = V_{10}(\omega).e^{j.(\omega.t+\varphi_2)} \qquad \text{and} \qquad \tilde{V}_2(\omega, t) = V_{20}(\omega).e^{j.(\omega.t+\varphi_4)} \qquad \text{(2a, b)}$$

where F_{10}, F_{20}, V_{10} and V_{20} are the amplitudes; and
φ_1, φ_2, φ_3 and φ_4 are the phases of the waveforms.

The four-pole parameters are designated as A, B, C and D, and the performance of the mount is defined by the following two equations:

$$\tilde{F}_1 = A.\tilde{F}_2 + B.\tilde{V}_2 \qquad \text{and} \qquad \tilde{V}_1 = C.\tilde{F}_2 + D.\tilde{V}_2 \qquad \text{(3a, b)}$$

Using equations (1) and (2), equations (3) may be expressed independently of time as:

$$F_{10}(\omega).e^{j.\varphi_1} = A.F_{20}(\omega).e^{j.\varphi_3} + B.V_{20}(\omega).e^{j.\varphi_4} \qquad \text{(4)}$$

$$V_{10}(\omega).e^{j.\varphi_2} = C.F_{20}(\omega).e^{j.\varphi_3} + D.V_{20}(\omega).e^{j.\varphi_4} \qquad \text{(5)}$$

Equations (4) and (5) may be written as:

$$F_1(\omega)=A.F_2(\omega)+B.V_2(\omega) \qquad \text{and} \qquad V_1(\omega) = C.F_2(\omega) + D.V_2(\omega) \qquad \text{(6a, b)}$$

where $F_1(\omega)=F_{10}(\omega).e^{j.\varphi_1}$, $\qquad F_2(\omega) = F_{20}(\omega).e^{j.\varphi_3}$,
$V_1(\omega) = V_{10}(\omega).e^{j.\varphi_2}$ $\qquad$ and $\qquad V_2(\omega) = V_{20}(\omega).e^{j.\varphi_4}$

Expressed in matrix form, equations (6) become:

$$\begin{bmatrix} F_1 \\ V_1 \end{bmatrix} = \begin{bmatrix} A & B \\ C & D \end{bmatrix} \cdot \begin{bmatrix} F_2 \\ V_2 \end{bmatrix}$$

(7)

Therefore the four-pole parameters are complex quantities, functions of ω and are time independent. The values of the parameters are the same as their instantaneous values and may be expressed as $A = A(\omega)$, $B = B(\omega)$, $C = C(\omega)$ and $D = D(\omega)$.

The four-pole parameters are determined individually by considering the following two special cases:

Case (1), for which the output side is blocked, i.e. $V_2 = 0$:

$$A = \left.\frac{F_1}{F_2}\right|_{V_2=0} \quad \text{and} \quad C = \left.\frac{V_1}{F_2}\right|_{V_2=0}$$

(8a, b)

Case (2), for which the output side is unrestrained, i.e. $F_2 = 0$:

$$B = \left.\frac{F_1}{V_2}\right|_{F_2=0} \quad \text{and} \quad D = \left.\frac{V_1}{V_2}\right|_{F_2=0}$$

(9a, b)

A port is defined as a pair of terminals giving external access to the mechanical system under study. Equation (7) may be solved for F_2 and V_2, by considering F_2 and V_2 as the input port and F_1 and V_1 as the output port, the signs of F_1 and F_2 being reversed. The signs of the forces must be reversed because F_1 is the force applied to the isolator, whereas F_2 is the force applied by the isolator. The force applied to the isolator is reversed in sign to the force applied by the isolator, by the principle of reactive forces. This yields the following equation:

$$\begin{bmatrix} F_2 \\ V_2 \end{bmatrix} = \frac{1}{\Delta} \cdot \begin{bmatrix} D & B \\ C & A \end{bmatrix} \cdot \begin{bmatrix} F_1 \\ V_1 \end{bmatrix}$$

(10)

where Δ is the determinant of the matrix $\begin{bmatrix} A & B \\ C & D \end{bmatrix}$,

i.e. $\Delta = A.D - B.C$

3

If Maxwell's law of reciprocal deflections is assumed to apply to the system, then it follows that the transfer impedance or mobility between any two ports is independent of which port is treated as the input or output [5]. Considering the above two cases of input and output ports that gave rise to equations (7) and (10), we have equality for the two blocked transfer mobilities, i.e.:

$$\frac{V_1}{F_2}\bigg|_{V_2=0} = \frac{V_2}{F_1}\bigg|_{V_1=0} \tag{11}$$

Solving equation (11) using equations (7) and (10) gives:

$$A.D - B.C = 1 \tag{12}$$

For the case of symmetric isolators i.e. those that behave the same if the input and output ports are interchanged, then interchanging these ports gives:

$$\begin{bmatrix} F_2 \\ V_2 \end{bmatrix} = \begin{bmatrix} A & -B \\ -C & D \end{bmatrix} \cdot \begin{bmatrix} F_1 \\ V_1 \end{bmatrix} \tag{13}$$

Solving equations (7) and (13) gives:

$$A = D \tag{14}$$

Equations (12) and (14) mean that there are only two independent four-pole parameters needed to be measured for a symmetric isolator in order to completely characterise it.

2.1 Impedance, Mobility and Inertance

Alternate functions commonly employed to describe isolator performance are the instantaneous blocked transfer inertance, impedance and mobility, designated respectively as I, Z and H and given by the following equations:

$$I = \frac{\mathcal{A}_1}{F_2}\bigg|_{V_2=0} \; ; \qquad Z = \frac{F_2}{V_1}\bigg|_{V_2=0} \qquad \text{and} \qquad H = \frac{V_1}{F_2}\bigg|_{V_2=0} \tag{15a, b, c}$$

where $\mathcal{A}_1$ is the instantaneous input acceleration, i.e. $\mathcal{A}_1 = j.\omega.V_1$

4

Combining equations (8) and (15) gives the instantaneous blocked transfer functions in terms of the four-pole parameter C:

$$I = j.\omega.C; \qquad\qquad Z = \frac{1}{C} \qquad \text{and} \qquad H = C \qquad \text{(16a, b, c)}$$

2.2 Effectiveness

Consider that the isolator, having four-pole parameters A, B, C and D, is placed between a vibration source and a foundation, as shown in Fig. 2(a). Let the driving point mobilities of the source and the foundation, measured at their connection points with the isolator, be H_1 and H_2 respectively, which are functions of frequency only. The velocities at the source / isolator and isolator / foundation interfaces are V_1 and V_2 respectively. The force exerted by the source on the isolator is F_1, and that of the isolator on the foundation is F_2. As before, equation (7) applies. Let V_0 be the free velocity of the source at the connection point, i.e. the source's unrestrained velocity. With the isolator connected, this instantaneous velocity changes to V_1, and by the principle of superposition, V_1 is the sum of the free velocity V_0 and the motion due to the resisting force of the isolator. This resisting force is $-F_1$, and produces a velocity of $H_1.(-F_1)$, and therefore:

$$V_1 = V_0 - H_1.F_1 \tag{17}$$

Additionally:

$$V_2 = H_2.F_2 \tag{18}$$

Solving equations (7), (17) and (18) to obtain V_2 and F_2 in terms of H_1 and H_2 gives the following relationships:

$$V_2 = \frac{V_0.H_2}{A.H_1 + B.H_1.H_2 + C + D.H_2} \tag{19}$$

$$F_2 = \frac{V_0}{A.H_1 + B.H_1.H_2 + C + D.H_2} \tag{20}$$

Now consider the situation that the source and foundation are directly connected, as shown in Fig. 2(b). In this situation:

$$V_1' = V_2' \qquad \text{and} \qquad F_1' = F_2' \qquad\qquad (21a, b)$$

Similarly to the above, let the free source velocity be V_0. Then the resultant motion V_1' is the sum of V_0 and the motion due to the resisting force, $-F_2$, exerted by the foundation on the source. Thus:

$$V_1' = V_0 - H_1 . F_1' \qquad\qquad (22)$$

and also:

$$V_2' = H_2 . F_2' \qquad\qquad (23)$$

Solving equations (21), (22) and (23) for V_2' and F_2':

$$V_2' = \frac{V_0 . H_2}{H_1 + H_2} \qquad\qquad (24)$$

$$F_2' = \frac{V_0}{H_1 + H_2} \qquad\qquad (25)$$

Define the effectiveness of isolation, E, as the ratio between the foundation velocity (or force) obtained when the source and foundation are directly connected i.e. Fig 2(b), and the foundation velocity (or force) obtained with the isolator included i.e. Fig. 2(a). Therefore, from equations (19) and (24), E may be expressed in terms of the four-pole parameters and the source and foundation mobilities, as follows:

$$E = \frac{V_2'}{V_2} = \frac{A.H_1 + B.H_1.H_2 + C + D.H_2}{H_1 + H_2} \qquad\qquad (26a, b)$$

The insertion loss, L, is defined as the magnitude of E expressed in dB:

$$L = 20.\log_{10} . \left| \frac{A.H_1 + B.H_1.H_2 + C + D.H_2}{H_1 + H_2} \right| \qquad\qquad (27)$$

Both E and L are functions of ω. For symmetric isolators, by combining equations (14) and (27), we obtain:

$$L = 20.\log_{10} . \left| A + \frac{B.H_1.H_2}{H_1 + H_2} + \frac{C}{H_1 + H_2} \right| \qquad\qquad (28)$$

At low frequencies the most significant of the three terms in equation (28) is generally found to be $C/H_1 + H_2$. Therefore at low frequencies to ensure good isolator effectiveness, the following inequality should hold true:

$$|C| \gg |H_1 + H_2| \tag{29}$$

From equation (16), the inequality (29) may be expressed as:

$$|H| \gg |H_1 + H_2| \tag{30}$$

The condition (30) means that in practice for good effectiveness at low frequencies the foundation needs to be very stiff when compared to the isolator, or the isolator needs to be very flexible compared to the foundation.

3. Experimental Method

The dynamic properties of vibration isolators are dependent upon the pre-load on the isolator, and so measurements should be made with a pre-load similar to the level that will be experienced in service. This means that the free situation $F_2 = 0$, embodied in equations (9), cannot be met. However the blocked situation $V_2 = 0$, can be satisfied with a blocking arrangement, thus allowing the measurement of parameters A and C to be accomplished using equations (8).

Verheij [7] describes a method for determining the acoustic properties of a resilient mounting in terms of its blocked transfer function, defined as the force out divided by the input acceleration. This paper follows Verheij's general experimental approach but characterises the dynamic properties of isolators in terms of their four-pole parameters.

An arrangement for measuring the blocked parameters is shown schematically in Fig. 3. The test isolator is held between two masses M_1 and M_2, which are assumed to behave as rigid bodies in the test frequency range (this assumption will be discussed later). The instantaneous blocking force F_2 is computed by measuring the acceleration $\mathcal{A}_2$ of the blocking mass M_2. Although this appears contradictory, Verheij [7] shows that under certain conditions a large mass supported on very soft mounts may be considered as effectively blocked. Thus:

$$F_2 = M_2 . \mathcal{A}_2 \quad \text{for } V_2 \approx 0 \tag{31}$$

7

The upper mass is driven by the two vibrators via stingers, and provides the input dynamic excitation to the upper side of the test isolator. It also transfers a pre-load to the test isolator to simulate the static load of shipboard machinery. The pre-load is adjustable and is applied from the air bag located above the excitation mass. The vibrators are considered to be effectively decoupled from the test frame.

The blocking mass defines the boundary condition on the lower side of the test isolator. Four air bags are positioned beneath the blocking mass, and are used to support it, the test isolator and the pre-load (including the excitation mass). The values of the masses and rotational inertias of the two blocks are sufficiently large to ensure that the six natural frequencies of each of the two mass mounting combinations, if installed on rigid foundations, are far lower than the lowest frequency of interest.

It is assumed that the orthogonal components of motion are uncoupled or only weakly coupled, and so for each orthogonal direction the four-pole parameters may be considered as independent. Normally the primary direction of interest is the axial, i.e. vertical, and the following discussion is restricted to this direction.

As previously defined, F_1 is the input force exerted by the excitation mass on the test isolator, and F_2 is the output force exerted by the test isolator on the blocking mass. As in the previous discussion, equation (7) applies. Let F_a and F_b be the sinusoidal forces exerted on the excitation mass by the two vibrators at the angular frequency of ω. $\mathcal{A}_1$ and V_1 are the acceleration and velocity at the excitation mass / test isolator interface, and $\mathcal{A}_2$ is the acceleration at the blocking mass / test isolator interface. We have:

$$F_1 = F_a + F_b - M_1 . \mathcal{A}_1 \tag{32}$$

$$F_2 = M_2 . \mathcal{A}_2 \tag{33}$$

From equation (8):

$$A = \left. \frac{F_1}{F_2} \right|_{V_2 \approx 0} \quad \text{and} \quad C = \left. \frac{V_1}{F_2} \right|_{V_2 \approx 0} \tag{34a,b}$$

Solving equations (12), (14), (32), (33) and (34) gives:

$$A = D = \left. \frac{F_a + F_b - M_1 . \mathcal{A}_1}{M_2 . \mathcal{A}_2} \right|_{V_2 \approx 0} \tag{35}$$

$$C = \frac{\mathcal{A}_1}{j.\omega.M_2.\mathcal{A}_2}\bigg|_{V_2 \approx 0} \tag{36}$$

$$B = \frac{A.D - 1}{C} \tag{37}$$

Therefore the four-pole parameters may be determined experimentally by measuring F_a, F_b, $\mathcal{A}_1$ and $\mathcal{A}_2$.

4. General Description of VITF

Using the general approach outlined above the vibration isolator test facility was designed and developed at the Aeronautical and Maritime Research Laboratory.

4.1 Physical

The test rig used is shown in Fig. 4. The input forces are generated by the two electrodynamic air cooled vibrators which in this case are operated in phase with each other. The arrangement of two vibrators allows them to be driven either in or out of phase, and for vertical motion the vibrators are connected for in phase actuation. Optoelectronic limit sensors were developed to minimise possible damage from over travel of the vibrators.

The excitation and blocking masses are regular cylinders having diameters of 296 mm and 942 mm and masses of 54.8 kg and 1076 kg, respectively. The rig has a moveable crosshead to allow testing of isolators with differing heights. The pre-load is supplied from the upper air bag, and may be varied to provide static loads up to 60 kN. The pre-load is a function of the air pressure and compressed operating height of the air bag and is determined from previous calibration of the air bag.

The lower four air bags, positioned beneath the blocking mass on a pitch circle of 732 mm, have a total supporting capability of 120 kN and may be pressure adjusted individually to ensure that the blocking mass is horizontal.

To increase the flexibility of the test rig three additional cylindrical masses were manufactured, having masses of 576, 197 and 100 kg. The 576 and 197 kg masses may be used as blocking masses for small capacity isolators, where the force levels required to produce measurable results on the 1076 kg mass exceed the isolator's capacity. They also offer higher frequency limits because of their higher structural modes. The 100 kg mass may be used as an excitation mass for very stiff isolators, where the rigid body

frequency of the 54 kg excitation mass is high enough to fall within the test frequency range.

To allow low level accelerometer measurements to be made with confidence, it was necessary to minimise structure and air borne extraneous acoustic vibrations. This was achieved by reducing the coupling of the test facility to its surroundings, and running the vibrators without forced air cooling by derating their force capability.

The reduced coupling was implemented by mounting the test facility on a 3 x 3 x 1 m reinforced concrete seismic mass supported on air springs. There are four seismic mass air springs, and the air springs are connected to accumulators to increase their air capacities and so reduce their stiffnesses. Two of the air springs are connected together and to an accumulator double the size of the other two accumulators. This arrangement effectively provides a three support system, which is necessary to preserve stability. The mass of the seismic mass is 21.8 t and the total mass of the test facility and seismic mass, excluding the two vibrators and test isolator, is 23.9 t. The natural frequency of the test rig / seismic mass and supporting air springs system was measured and found to be 1.1 Hz.

The decoupling was further improved by removing the vibrators from the main frame of the test facility and suspending them from a separate frame with soft rubber springs. This frame was supported separately to the seismic mass, and effectively decoupled the vibrators from the test rig, but still provided input forcing functions from the vibrators to the isolator via the stingers and excitation block.

4.2 Instrumentation

To determine the four-pole parameters from equations (35) to (37), it was necessary to measure F_a, F_b, $\mathcal{A}_1$ and $\mathcal{A}_2$. F_a and F_b were measured using force transducers located between the stingers and the excitation mass. $\mathcal{A}_1$ and $\mathcal{A}_2$ were experimentally found by using a pair of symmetrically positioned accelerometers on each of the two masses, and averaging their outputs. The two excitation mass accelerometer outputs were designated as $\mathcal{A}_{1a}$ and $\mathcal{A}_{1b}$ and the two blocking mass accelerometer outputs were designated as $\mathcal{A}_{2a}$ and $\mathcal{A}_{2b}$.

The upper frequency limit of the test facility was determined practically by its ability to sense low values of $\mathcal{A}_2$ and by the modal properties of the blocking mass. The structural modal characteristics are discussed in section 5.2. Specialised high sensitivity and low noise accelerometers and charge amplifiers were acquired to measure $\mathcal{A}_{1a}$, $\mathcal{A}_{1b}$, $\mathcal{A}_{2a}$ and $\mathcal{A}_{2b}$. Each accelerometer had a nominal sensitivity of 31.6 pC/ms^2, and each accelerometer/charge amplifier combination produced an output sensitivity of 10 V/ms^2, had a lower dynamic limit of 200 μm/s^2 (rms with

signal-to-noise ratio > 6 dB and over the range 2 Hz to 22 kHz) and had a frequency response flat to within ±5%, over the range from 0.2 Hz to 2.8 kHz.

A digital computerised eight channel FFT spectrum/network analyser was used to control the test, and to acquire and analyse the data. It generated an output signal S_0 that controlled the power amplifier supplying the vibrators, and so controlled the vibratory forcing function applied to the excitation mass. This control may also be a closed loop, by feeding back the monitored excitation mass acceleration to the analyser. The analyser has been programmed to conduct swept sine measurements of the signals F_a, F_b, $\mathcal{A}_{1a}$, $\mathcal{A}_{1b}$, $\mathcal{A}_{2a}$, $\mathcal{A}_{2b}$ and S_0. It produced a sinusoidal control signal that swept across a frequency band with selectable lower and upper limits in a selectable number of steps that are logarithmically spaced. At each frequency the analyser determined the frequency response functions of the measured parameters by integrating the acquired data over a selectable number of cycles of the driving frequency. The signal S_0 was specified as the reference, and all other parameters were measured in terms of their moduli and phase angles relative to S_0.

5. Modal Analyses

The test rig exhibited rigid body and structural modes of vibration. The rigid body modes have been analysed by considering the system to be represented by point masses separated by elements having dynamic stiffnesses. The structural modes have been considered by experimentally investigating the blocking mass, excitation mass and supporting structure.

5.1 Rigid Body Modes

In order to investigate the low frequency rigid body modes, the system may be modelled as a simple linear three degrees-of-freedom mass-spring system as shown in Fig 5. There are three point masses M_1, M_2 and M_3 and four linear springs of dynamic stiffnesses K_1, K_2, K_3 and K_4.

M_1 represents the seismic mass and mass contribution from the main frame of the test rig, M_2 represents the blocking mass and mass contribution from the lower air bags and test isolator, and M_3 represents the excitation mass and mass contribution from the test isolator and pre-loading air bag. The seismic mass's supporting air bags are represented by the massless spring K_1, the blocking mass's supporting air bags by the spring K_2, the test isolator by the spring K_3 and the pre-loading air bag by the spring K_4. By solving the equations of motion for the three masses, it may be shown that the

three natural frequencies of this model, denoted as ω_1, ω_2 and ω_3, are given by solving the frequency equation:

$$\omega^6 - \alpha_4 \cdot \omega^4 + \alpha_2 \cdot \omega^2 - \alpha_0 = 0 \tag{38}$$

where
$$\alpha_0 = \frac{K_1 \cdot K_2 \cdot K_3 + K_1 \cdot K_2 \cdot K_4 + K_1 \cdot K_3 \cdot K_4}{M_1 \cdot M_2 \cdot M_3}$$

$$\alpha_2 = \frac{M_1 \cdot (K_2 \cdot K_3 + K_3 \cdot K_4 + K_2 \cdot K_4) + M_2 \cdot (K_1 + K_2) \cdot (K_3 + K_4) +}{M_1 \cdot M_2 \cdot M_3}$$
$$\frac{+ M_3 \cdot (K_1 \cdot K_2 + K_2 \cdot K_3 + K_3 \cdot K_1)}{M_1 \cdot M_2 \cdot M_3}$$

$$\alpha_4 = \frac{K_1 \cdot M_2 \cdot M_3 + K_2 \cdot (M_1 + M_2) \cdot M_3 + K_3 \cdot M_1 \cdot (M_2 + M_3) + K_4 \cdot M_1 \cdot M_2}{M_1 \cdot M_2 \cdot M_3}$$

Using the following values for the dynamic spring constants derived for a representative test isolator:

$K_1 = 1.25.10^6$ N/m, $K_2 = 3.61.10^5$ N/m, $K_3 = 1.31.10^6$ N/m and $K_4 = 1.05.10^5$ N/m.

Allowing for the mass contributions of the air bags, transducers and stinger attachments, the mass values are:

$M_1 = 23.9$ t, $M_2 = 1082$ kg and $M_3 = 55.8$ kg.

With these values for the spring constants and masses, equation (38) yields the natural frequencies as $f_1 = 1.13$ Hz, $f_2 = 3.27$ Hz and $f_3 = 25.9$ Hz. The second and third frequencies agree closely with the experimentally determined values of 3.3 and 26 Hz.

5.1.1 Lower Frequency Limit

The lower frequency limit is determined by the rigid body modal behaviour of the test rig, and the upper frequency limit by the modal properties of the blocking mass. The rigid body modal behaviour depends upon the pre-load and the test isolator, and the values of F_1 and F_2 are inferred from the measurements of the accelerations of the excitation and blocking masses.

According to Verheij [7] the excitation mass / test isolator sub-system, when mounted on a rigid foundation should have an axial natural frequency well below the frequency range of measurement. This natural frequency of the sub-system is approximately equal to the frequency f_3 for the system mode having the excitation and blocking

masses out of phase with each other. Since f_3 is greater than f_1 and f_2, the lower frequency limit of measurement is controlled by f_3. A practical lower limit is considered to be twice the frequency f_3, which for the representative isolator considered is approximately 60 Hz.

In a similar fashion the practical lower limit using the 576 kg blocking mass with the representative isolator will be the same. This follows from the solution of the natural frequencies from equation (38) as $f_1 = 1.14$ Hz, $f_2 = 4.34$ Hz and $f_3 = 26.4$ Hz.

5.2 Structural Modes

Modal analyses were conducted on the blocking mass, excitation mass and supporting structure of the test rig. The analyses were performed with the test rig set up to investigate a representative test isolator under normal service pre-load. The masses and supporting structure were in turn excited with a modal hammer and the response measured using an accelerometer located at one position on the mass or structure under investigation. The excitation point was varied over the surface of the mass or structure, and corresponding frequency response functions and coherence functions measured and stored using a fast Fourier transform (FFT) analyser. Each stored frequency response function was obtained by averaging the results of eight hammer excitations.

5.2.1 Blocking Mass

A detailed modal analysis was conducted on the blocking mass. The blocking mass was excited using a modal hammer and the response measured using an accelerometer positioned at one location. The excitation point was varied over the block at 25 locations. At each location eight frequency response functions were collected using force-exponential windowing, and these frequency response functions were then averaged to produce one frequency response function for storage and analysis. A dual channel FFT analyser was employed for this purpose. The various excitation points are shown in Fig. 6, and the response was measured at point 1 in all cases. A typical frequency response function (FRF) is shown in Fig. 7, and the peaks in the frequency response function correspond to resonant frequencies.

The frequency response function data was then analysed using the Imperial College Analysis Testing and Software package developed by the Imperial College [8]. The data was analysed using the Imperial College Analysis Testing and Software multiple frequency response function technique Global-M, which is a modal parameter extraction method using batch processing of the frequency response functions. This yielded eleven modes of vibration in the frequency range of 20 Hz to 5 kHz. The resonant frequencies are listed in Table 1. The mode shapes are schematically shown in Figs 8 to 13.

Analysis of these modal shapes showed that they would generate minimal structural modal contribution to the sensed acceleration signals if the accelerometers were located along the diameters joining, and at or close to, the points 10 and 14; or 12 and 16 in Fig. 6. These points are located approximately at nodes of the first four mode shapes, and so will minimise errors introduced from flexures of the block at its natural frequencies.

For minimal effect of the structural modes on the motion of the test isolator, there should be a node located at the centre of the block. In analysing the mode shapes, it should be noted that the test isolator had a steel mounting plate of dimensions 210 x 410 x 35 mm attached to its base. Effectively there is a central node for the first mode. However, in the second and third modes there is an anti-node at the centre, and so the natural frequency of the second mode sets the upper frequency bound for testing. Therefore the upper frequency limit is 1555 Hz, and a practical limit is one half this frequency, which for the representative isolator considered is approximately 800 Hz.

The four supporting air bags are also symmetrically located along the nodal lines 8-16-24-25-20-12-4 and 2-10-18-25-22-14-6. The accelerometers were tried at different positions along these nodal lines and at or near to positions 10 and 14, with the same test set-up and the vibrators energised. The accelerometer positions that produced the minimal noise output were selected, and were on a pitch circle of radius 291 mm. The corresponding maximum noise floor value, measured over the frequency range of 20 Hz to 3.2 kHz, was 30 $\mu m/s^2$(rms). This indicates that the system performance of the test facility is at the limit of the accelerometer performance capability.

In a similar fashion the 576 kg blocking mass was investigated, and the upper frequency bound for testing purposes was found to be 1 kHz.

5.2.2 Excitation Mass and Frame

The modal properties of the excitation mass are less important than those of the blocking mass because the overall performance limitations are determined by the latter's modal properties and low acceleration levels. Using the same test set-up, frequency response functions were measured at ten points on the excitation block, in a manner similar to that described above for the blocking mass. The excitation points are shown in Fig. 14, and the driving stingers are located at points 9 and 10. For all cases the response was measured at point 1. The hammer excitation was applied from beneath for points 9 and 10, and was averaged around the response accelerometer for point 1. A typical resultant averaged frequency response function is given in Fig. 15. No significant resonant frequencies are evident within or near the blocking mass's frequency limits.

Frequency response functions were also measured at 28 key locations on the main frame of the test rig with the response monitored at position 1 (Fig. 14) on the

excitation mass, and position 1 (Fig. 6) on the blocking mass. A typical example of the resultant 28 averaged frequency response functions is shown in Fig. 16. Over the frequency range of 20 Hz to 1.5 kHz the frequency response functions of the main frame are at least 70 dB down in comparison with the frequency response functions of the blocking and excitation masses. Therefore the frequency response functions demonstrate that there is only weak coupling between the frame and the blocking and excitation masses, and no significant coupling is evident within or near the blocking mass's frequency limits.

6. Vibration Isolator Test

A representative isolator under pre-load was tested over the frequency range from 30 Hz to 1 kHz using the 576 kg blocking mass and the 54.8 kg excitation mass. The four-pole parameters were computed from the experimental results using equations (35) to (37), and the results are displayed in Fig 17.

The four-pole parameter C is the blocked transfer mobility and for low frequencies has a measured slope of 20 dB/decade and a phase angle of approximately 90 degrees. This indicates massless spring-like behaviour and is valid up to approximately 300 Hz. Furthermore, this spring-like characteristic implies that $F_1 \approx F_2$ and $V_1 \approx V_2$, and so from equations (8) and (14), $A = D \approx 1$ for a symmetric isolator. This approximation agrees with the measurements for low frequencies.

In the region from 100 to 200 Hz, the four-pole parameters A, B and D exhibit an anti-resonance type characteristic. Each of these parameter displays a pronounced dip in its magnitude curve, and a corresponding phase change of approximately 180 degrees. Parameters A and D change from approximately 0 to -180 degrees, and parameter B changes from approximately 90 to 270 degrees as the frequency increases through the anti-resonances. For the parameter A, the frequency of this phenomena is dependant upon the mass of the upper plate of the isolator and the dynamic stiffness of the elastomer. It appears to be due to a resonance of the isolator upper plate on the elastomer. The frequencies of the dips for parameters B and D then follow from equations (12) and (14).

At higher frequencies standing waves within the isolator are evident as indicated by the resonant type peaks in the moduli curves, for example the parameter C peak marked * in Fig. 17.

15

# 7. Conclusions

Vibration isolation mounts may be characterised in terms of their four-pole parameters, which are independent of the characteristics of other mechanical systems located before and after the isolator. Measurement of two independent parameters is sufficient to determine the dynamic properties of a symmetric isolator. The effectiveness of isolation depends upon the four-pole parameters of the mount and the mobilities of the vibration source and foundation.

The test facility has been developed and tests demonstrate that it is capable of investigating the acoustic transmission characteristics of flexible vibration isolating mounts for shipboard machinery. Key features of the test facility include the capability to sense low level parameters and the provision of a variable pre-load up to 60 kN. A typical ship machinery mount was tested in the test facility to obtain acoustic transmission data by determining its four-pole parameters.

Table 1: Mode frequencies

Mode number	Resonant frequency (Hz)
1	1027
2	1555
3	1775
4	2084
5	3063
6	3212
7	4390
8	4518
9	4612
10	4895
11	4624
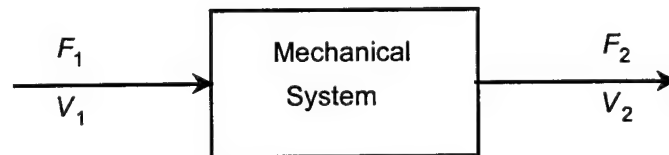
Figure 1: Mathematical model of isolation mount

(a) (b)
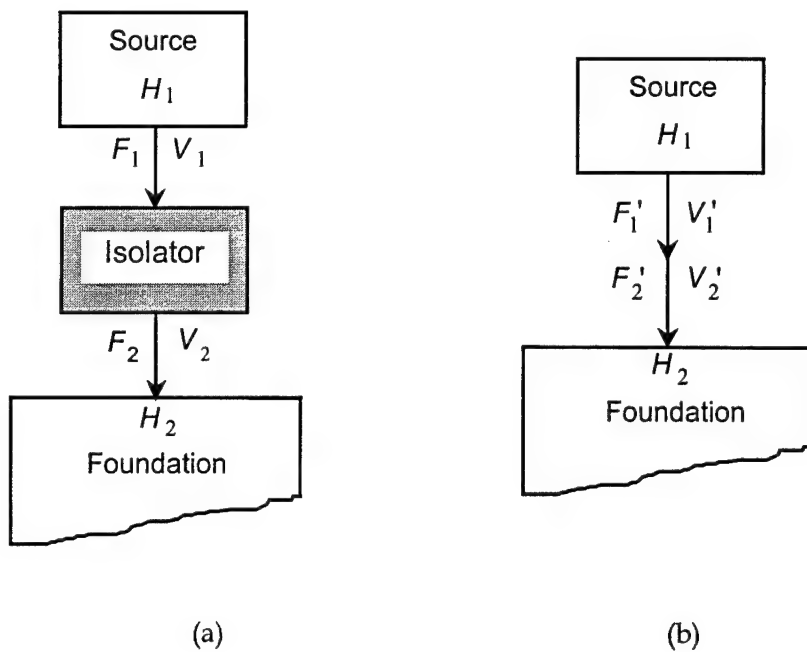
Figure 2: Isolator effectiveness
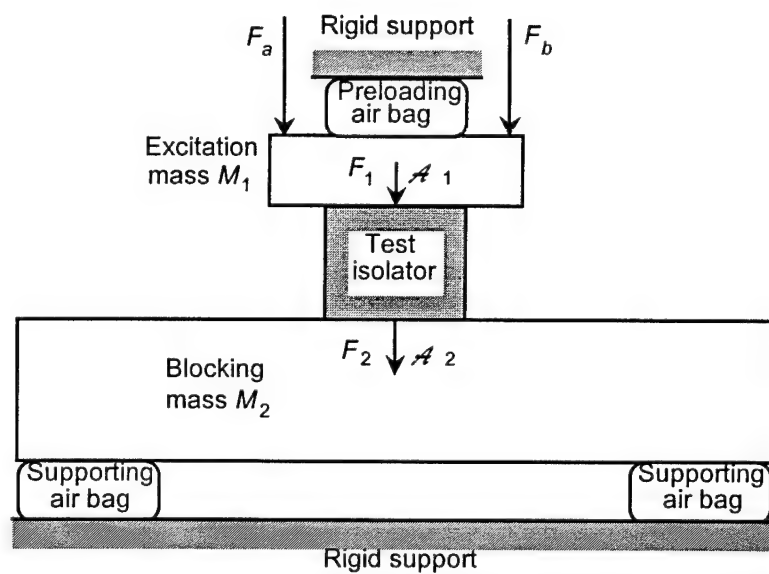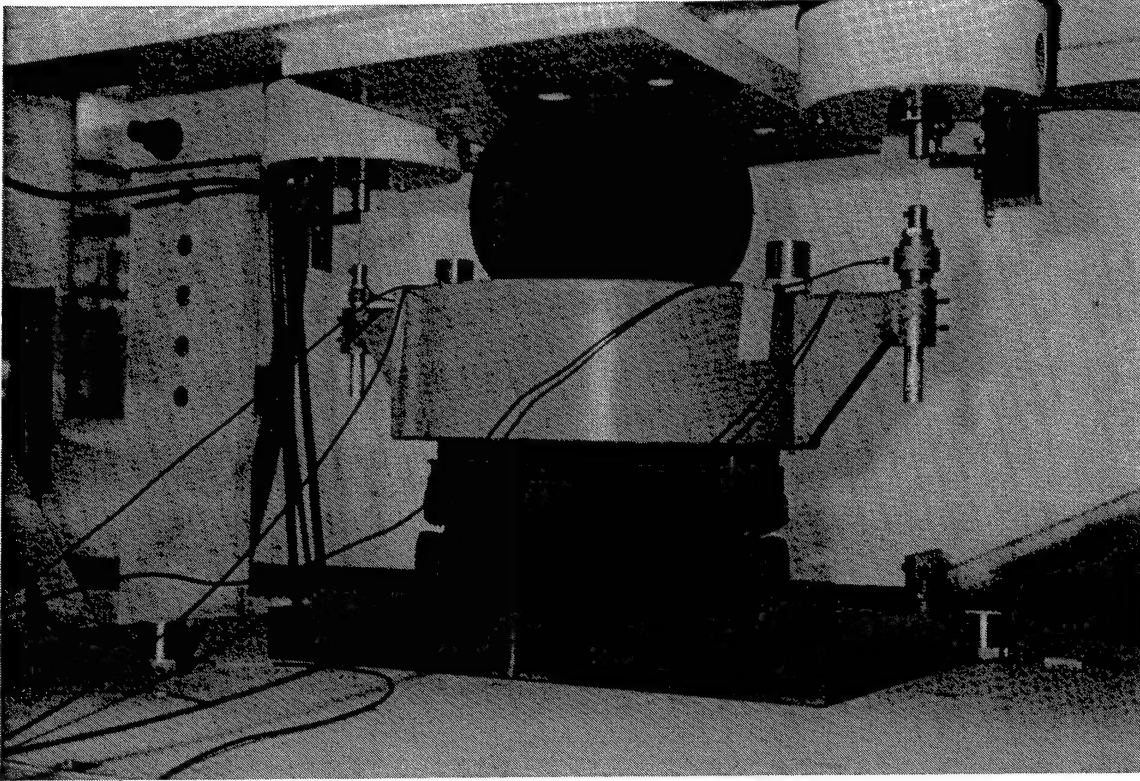

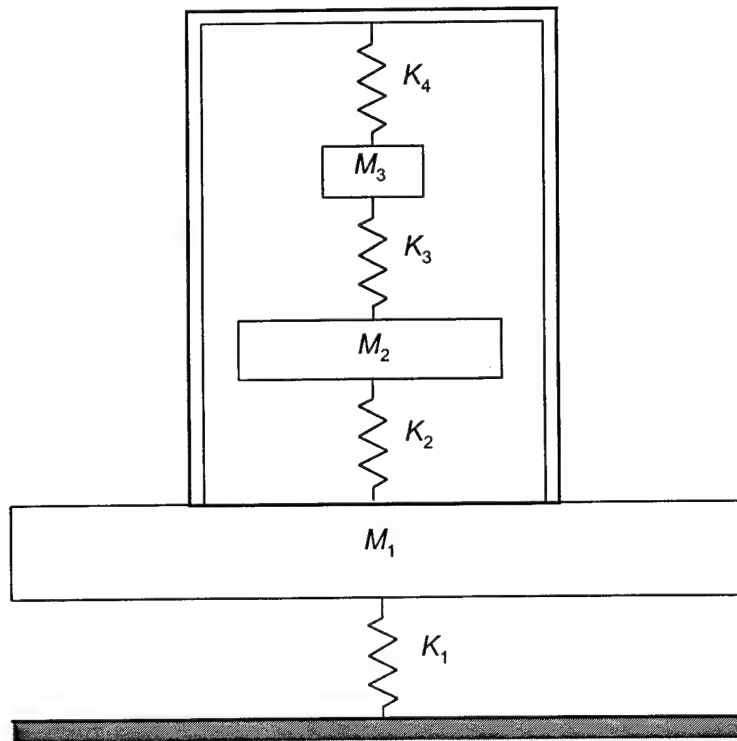*Figure 3: Schematic test arrangement*

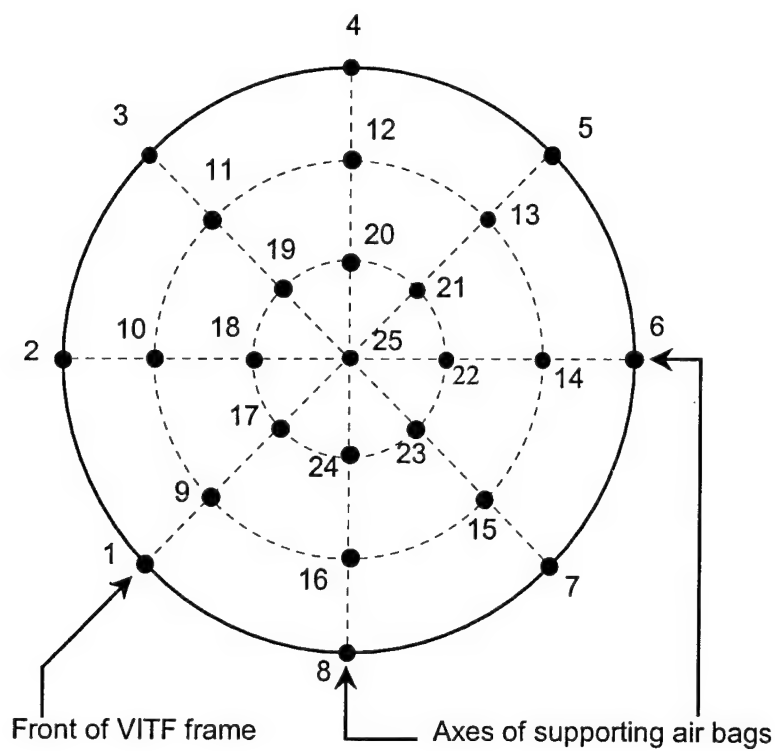Figure 4: Test set-up

Figure 5: Mass-spring model
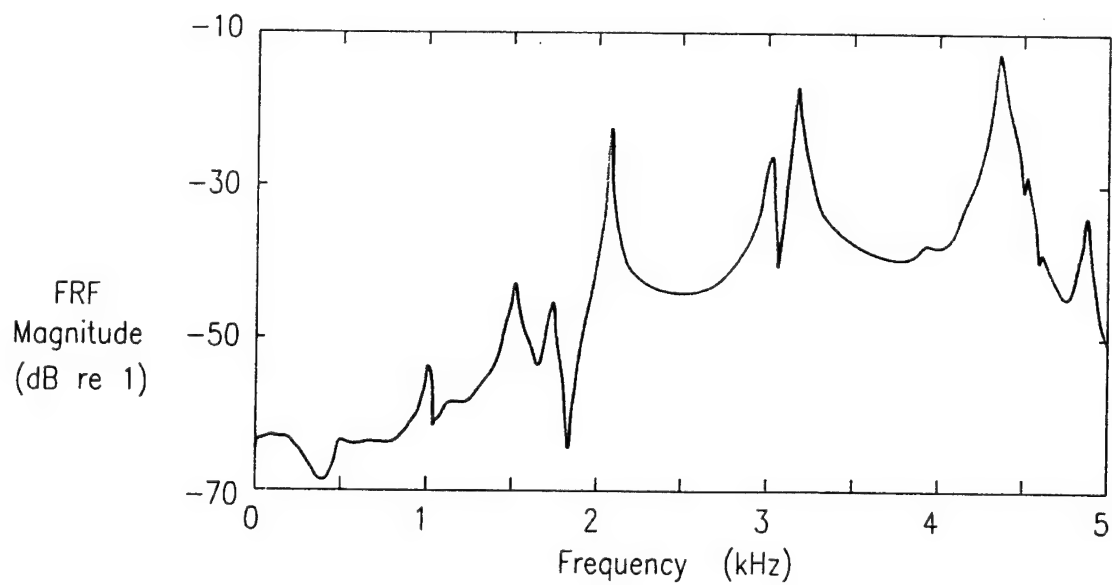
19

Figure 6: Measurement points on the blocking mass

Figure 7: Typical frequency response function for blocking mass
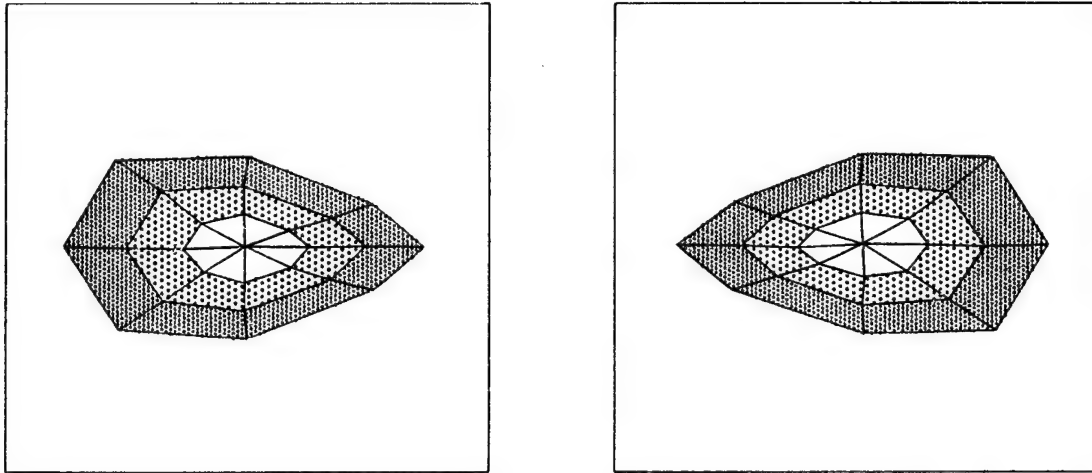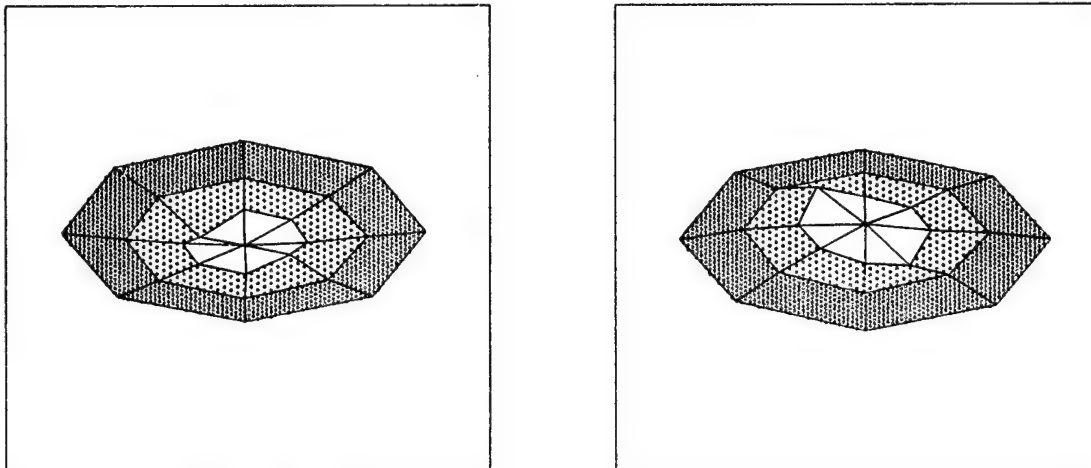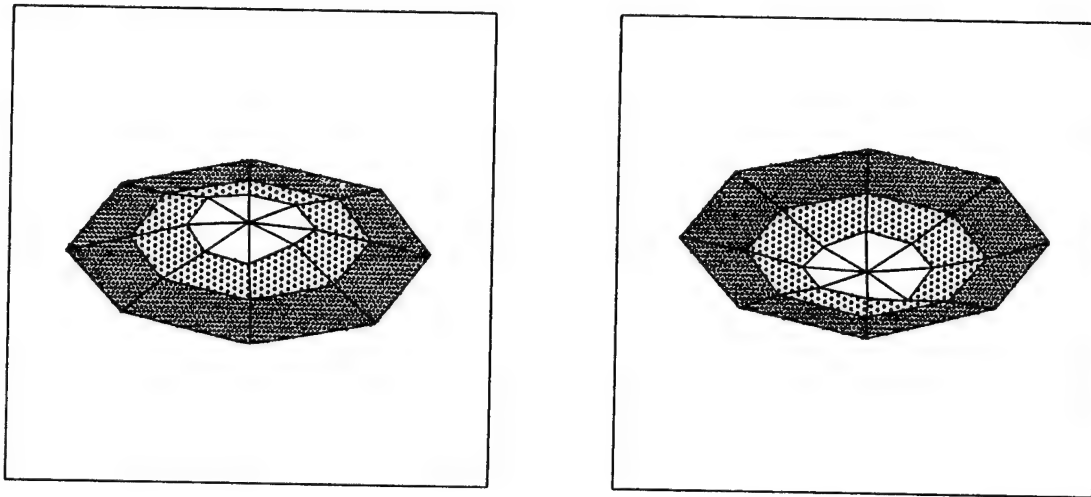
Figure 8: First mode shape of the blocking mass

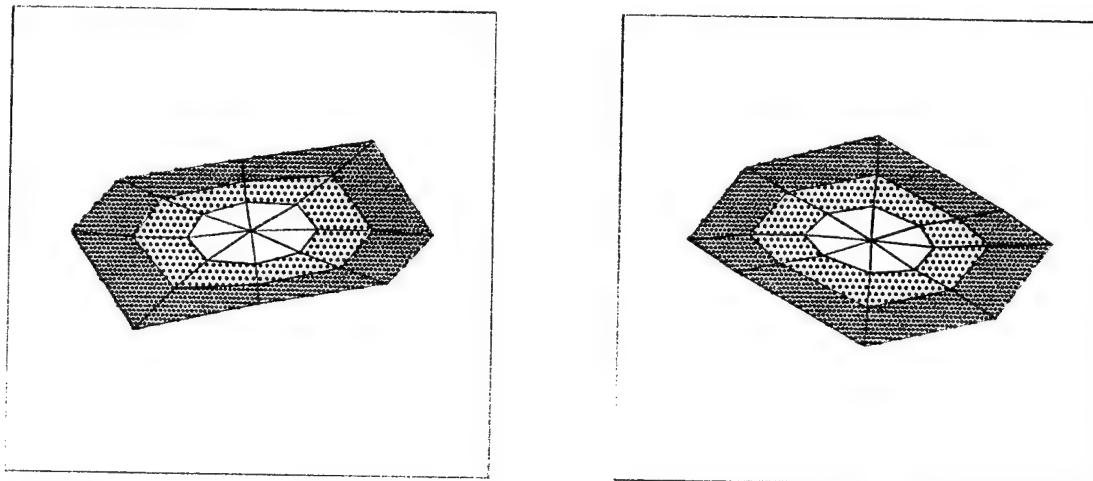*Figure 9: Second mode shape of the blocking mass*

Figure 10: Third mode shape of the blocking mass

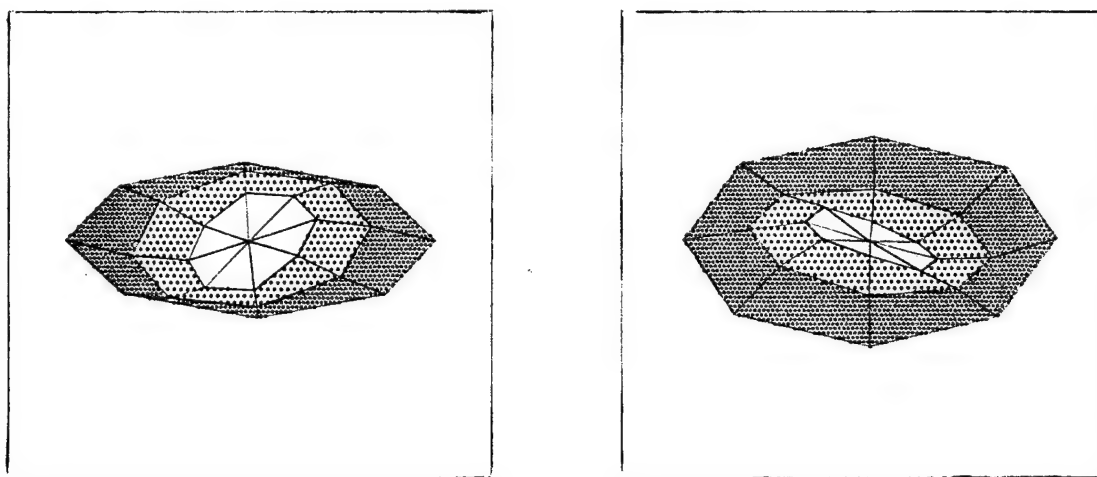Figure 11: Fourth mode shape of the blocking mass
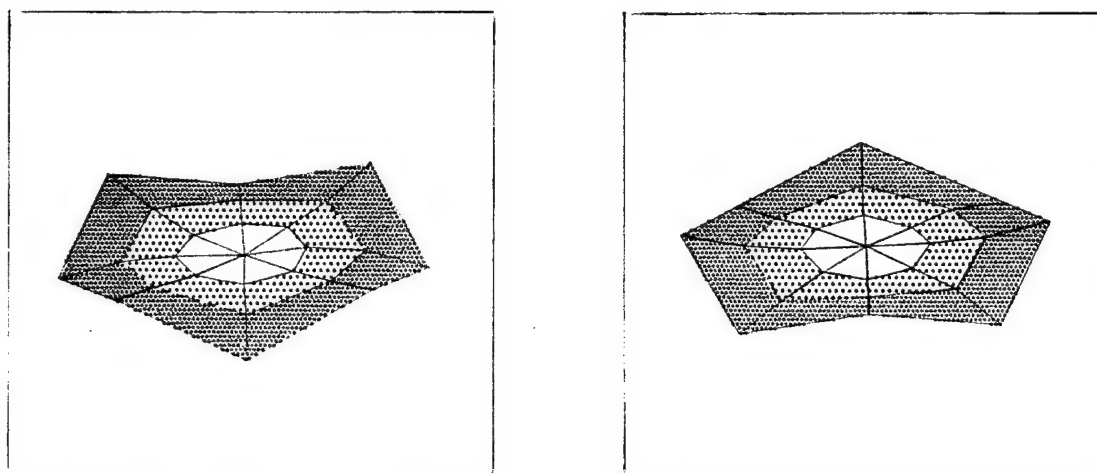
Figure 12: Fifth mode shape of the blocking mass
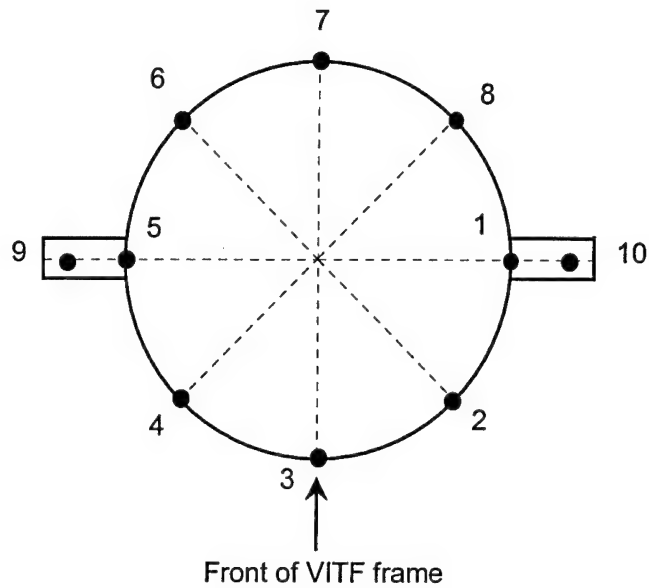

Figure 13: Sixth mode shape of the blocking mass

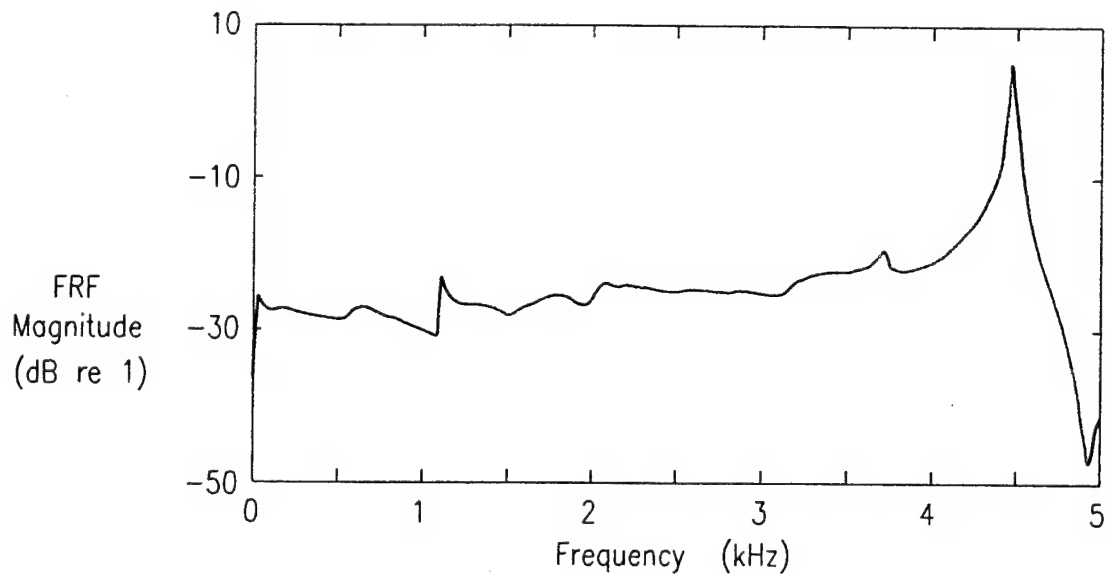*Figure 14: Measurement points on the excitation mass*

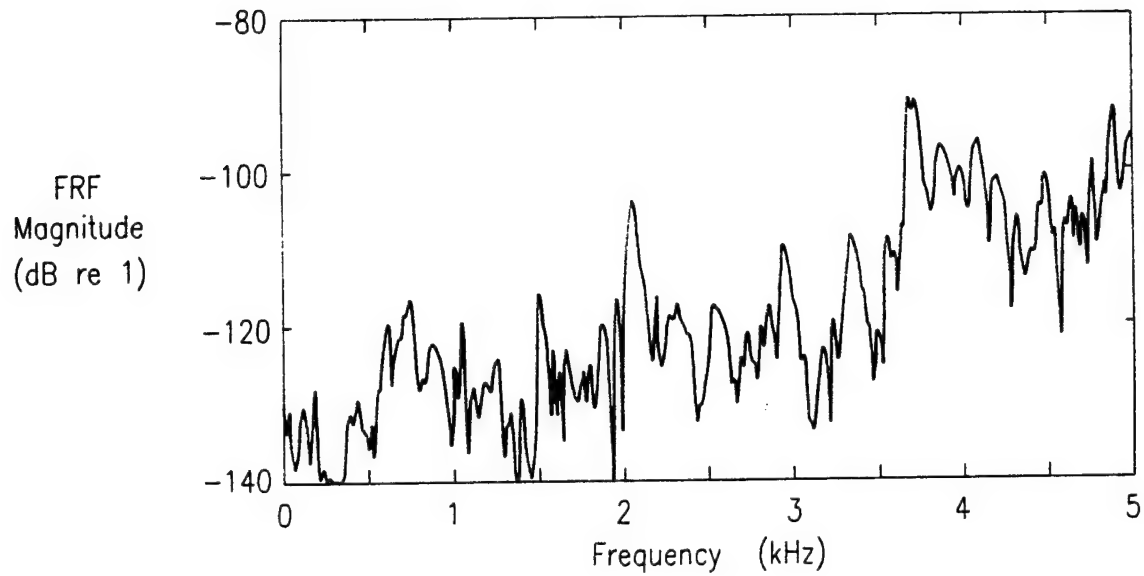*Figure 15: Typical frequency response function for excitation mass*

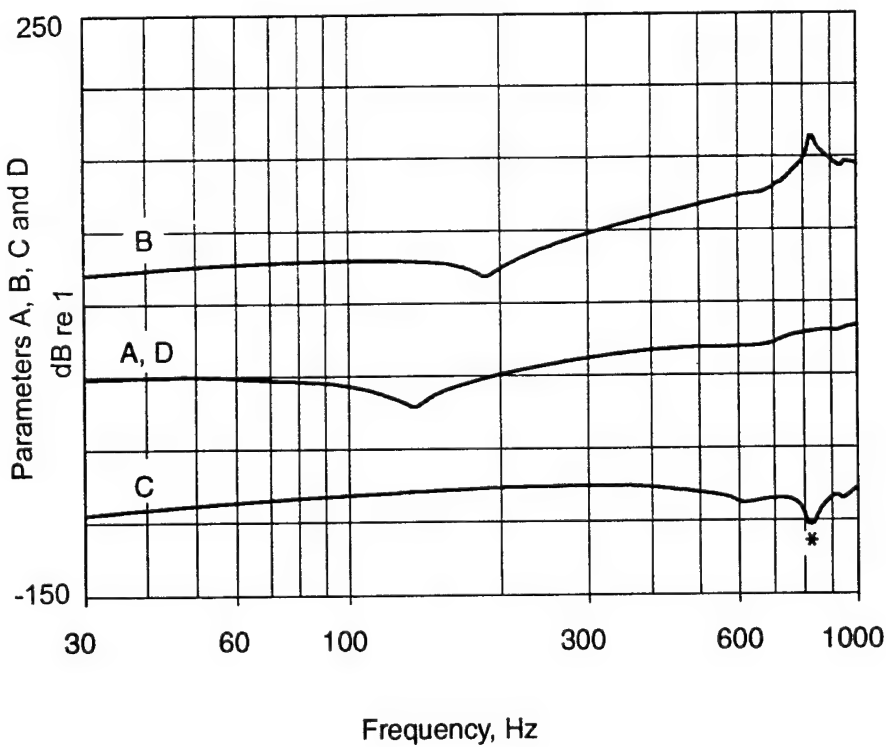Figure 16: Typical frequency response function for main frame of the test facility

Figure 17: Four-pole parameters of representative isolator

8. References

1. Dickens, J.D., Norwood, C.J., and Juniper, R.G., "Four Pole Parameter Characterisation of Isolator Acoustic Transmission Performance", Proc. Australian Acoustical Society Annual Conference, Glenelg, South Australia, pp. 110-117, November 9-10, 1993.

2. Jacobsen, F. and Ohlrich, M., "Vibrational power transmission from multipoint mounted machinery to supporting structure", The Acoustical Laboratory, Technical University of Denmark report 35, February 1986.

3. Molloy, C.T., "Use of Four-Pole Parameters in Vibration Calculations", Journal of the Acoustical Society of America 29, pp 842-853, vol. 29, no. 7, July 1957.

4. Norwood, C., "Vibration Isolator Properties and Performance Prediction", Odegaard & Danneskiold-Samsoe ApS report 87.199, December 1987.

5. Snowdon, J.C., "Mechanical Four-pole Parameters: Transmission Matrices", The Pennsylvania State University, Applied Research Laboratory report to the U.S. Naval Sea Systems Command, report no. TM 76-122, April 1976.

6. Snowdon, J.C., "Vibration isolation: Use and characterisation", Journal of the Acoustical Society of America, pp 1245-1274, vol. 66, no. 5, November 1979.

7. Verheij, J.W., "Multi-path sound transfer from resiliently mounted shipboard machinery", Ph.D. thesis, Institute of Applied Physics TNO-TH, Delft, 1982.

8. Imperial College Analysis Testing and Software (ICATS), "Integrated Software for Structural Dynamics" software package, Imperial College of Science, Technology and Medicine, Mechanical Engineering Department, London, March 1993.

9. Appendix A

List of Symbols

$\mathcal{A}$	acceleration
A, B, C, D	four-pole parameters
E	effectiveness of isolator
FFT	fast Fourier transform
F	force
H	mobility
I	inertance
j	$j = \sqrt{-1}$
K	dynamic stiffness
L	insertion loss of isolator
M	mass
V	velocity
ω	circular frequency
x, y, z	orthogonal axes of cartesian co-ordinate system
Z	impedance

DISTRIBUTION LIST

Vibration Isolator Test Facility

J.D. Dickens and C.J. Norwood

AUSTRALIA

DEFENCE ORGANISATION

Defence Science and Technology Organisation

Chief Defence Scientist
FAS Science Policy
AS Science Industry and External Relations
AS Science Corporate Management
} shared copy

Counsellor Defence Science, London (Doc Data Sheet only)
Counsellor Defence Science, Washington (Doc Data Sheet only)
Scientific Adviser to Thailand MRDC (Doc Data Sheet only)
Director General Scientific Advisers and Trials/ScientificAdviser Policy and Command
 (shared copy)
Navy Scientific Adviser
Scientific Adviser - Army Data Sheet (Doc and distribution list only)
Air Force Scientific Adviser
Director Trials

Aeronautical and Maritime Research Laboratory

Director
Chief, SSMD
J.C. Ritter
R. Juniper
J.D. Dickens
C.J. Norwood

Electronics and Surveillance Research Laboratory

Director

DSTO Library

Library Fishermens Bend
Library Maribyrnong
Australian Archives
Main Library DSTOS (2 copies)
Library, MOD, Pyrmont (Doc Data sheet only)

Defence Central

OIC TRS, Defence Central Library
Officer in Charge, Document Exchange Centre (DEC), 1 copy
*US Defence Technical Information Centre, 2 copies
*UK Defence Research Information Centre, 2 copies
*Canada Defence Scientific Information Service, 1 copy
*NZ Defence Information Centre, 1 copy
National Library of Australia, 1 copy
Defence Intelligence Organisation
Library, Defence Signals Directorate (Doc Data Sheet only)

<u>Army</u>

Director General Force Development (Land), (Doc Data only)
ABCA Office, G-1-34, Russell Offices, Canberra   (4 copies)

<u>Navy</u>

Director General Naval Warfare
Director General Force Development (Sea)
Director General Naval Engineering Services
Director General Naval Engineering Requirements
Director General Equipment Procurement
       Attn. Acoustsic Surveillance Systems and Tactical Array Sonar Systems
Director Naval Architecture
Director Marine Engineering
Submarine Project Director
SO (Science), Director of Naval Warfare, Maritime Headquarters Annex, Garden
      Island, NSW 2000. (Doc Data Sheet)

UNIVERSITIES AND COLLEGES

Australian Defence Force Academy
      Library
      Head of Aerospace and Mechanical Engineering
Deakin University, Serials Section (M list), Deakin University Library, Geelong, 3217
Senior Librarian, Hargrave Library, Monash University

OTHER ORGANISATIONS

NASA (Canberra)
AGPS

ABSTRACTING AND INFORMATION ORGANISATIONS
      INSPEC: Acquisitions Section Institution of Electrical Engineers
      Library, Chemical Abstracts Reference Service
      Engineering Societies Library, US
      American Society for Metals
      Documents Librarian, The Center for Research Libraries, US

INFORMATION EXCHANGE AGREEMENT PARTNERS
      Acquisitions Unit, Science Reference and Information Service, UK
      Library - Exchange Desk, National Institute of Standards and Technology, US

SPARES (10 copies)

DEFENCE SCIENCE AND TECHNOLOGY ORGANISATION DOCUMENT CONTROL DATA	1. PRIVACY MARKING/CAVEAT (OF DOCUMENT)

2. TITLE Vibration Isolator Test Facility	3. SECURITY CLASSIFICATION (FOR UNCLASSIFIED REPORTS THAT ARE LIMITED RELEASE USE (L) NEXT TO DOCUMENT CLASSIFICATION) Document (U) Title (U) Abstract (U)

4. AUTHOR(S) J.D. Dickens and C.J. Norwood	5. CORPORATE AUTHOR Aeronautical and Maritime Research Laboratory PO Box 4331 Melbourne Vic 3001

6a. DSTO NUMBER DSTO-TR-0357	6b. AR NUMBER AR-009-732	6c. TYPE OF REPORT Technical Report	7. DOCUMENT DATE June 1996

8. FILE NUMBER 510/207/0279	9. TASK NUMBER DST 93/139	10. TASK SPONSOR DST	11. NO. OF PAGES 27	12. NO. OF REFERENCES 8

13. DOWNGRADING/DELIMITING INSTRUCTIONS None	14. RELEASE AUTHORITY Chief, Ship Structures and Materials Division

15. SECONDARY RELEASE STATEMENT OF THIS DOCUMENT

Approved for public release

OVERSEAS ENQUIRIES OUTSIDE STATED LIMITATIONS SHOULD BE REFERRED THROUGH DOCUMENT EXCHANGE CENTRE, DIS NETWORK OFFICE, DEPT OF DEFENCE, CAMPBELL PARK OFFICES, CANBERRA ACT 2600

16. DELIBERATE ANNOUNCEMENT

No limitations

17. CASUAL ANNOUNCEMENT   Yes

18. DEFTEST DESCRIPTORS

Vibration damping; Acoustic transmission; Signatures; Ship signatures; Ship board machinery; Sonar detection; Vibrations; Vibration transmission

19. ABSTRACT
This report details the development of a vibration isolator test facility at the Aeronautical and Maritime Research Laboratory. The test facility was designed to investigate the acoustic transmission characteristics of resilient vibration isolating mounts for shipboard machinery. The characteristics of the isolators are described in terms of their four-pole parameters. Features of the test facility include the capability to sense low level motion and the provision of a variable pre-load up to 60 kN. A modal analysis was conducted with the boundary conditions that are experienced in an actual test situation. This revealed details concerning the influence of structural modes on the test measurements, and led to location of the sensing accelerometers which permitted data to be obtained out to 1 kHz with confidence. This report also describes the testing of a typical ship machinery mount in the test facility by determining the four-pole parameters of the vibration isolator.